

Spectroscopic investigation of the encapsulation and the reactivity towards NO of a Co(II)-porphyrin inside a cross-linked polymeric matrix

Svetoslava Vankova,^a Elena Groppo,^{*a} Mario Chiesa,^a Alessandro Damin,^a Claudia Barolo,^b Giuseppe Spoto^{*a} and Adriano Zecchina^a

Received 3rd December 2008, Accepted 3rd March 2009

First published as an Advance Article on the web 28th April 2009

DOI: 10.1039/b821714a

A highly dispersed cobalt(II) porphyrin (PhCo^{II}) encapsulated inside a highly cross-linked poly(4-ethylstyrene-co-divinylbenzene) matrix (St-DVB) is investigated by means of FTIR, Raman, UV-Vis and EPR spectroscopies. The adoption of the highly porous St-DVB support is the key factor in reaching an optimum porphyrin dispersion in undiluted conditions (~10 wt% of porphyrin). It is demonstrated that the encapsulated PhCo^{II} are characterized by the absence of any axial interactions involving the polymeric matrix, that can be considered a “non-coordinating” solvent. Finally, the permanent porosity of the encapsulating matrix allows gaseous molecules to reach the Co^{II} cations also in the absence of swellable solvents. In particular, the reactivity of the isolated Co^{II} porphyrin species towards nitric oxide (NO) is investigated, with possible implications in the understanding of the crucial role played by NO in biological systems.

1. Introduction

Metalloporphyrins are large macro-cyclic molecules which have found application as highly efficient oxidation,^{1–8} epoxidation^{2,9–13} and hydroxylation catalysts.^{14–17} In many cases their activity and selectivity closely resemble those of biological systems such as, for instance, cytochrome P-450: for this reason synthetic metalloporphyrins have been considered for some time as structural and mechanistic models for enzymes.^{11,18–24}

The use of metalloporphyrins in catalysis suffers, however, from some drawbacks, such as the difficulty of their recovery from the reaction medium (when used in heterogeneous conditions), chemical instability and tendency to form aggregates (dimers, trimers, *etc.*) when used in homogeneous conditions.²³ Dispersion and/or immobilization on solid supports can actually help to overcome some of these problems and also allows the extension of metalloporphyrins to technological fields other than catalysis, such as chemical sensors^{25–29} and solar cells.^{30–32}

Among the approaches adopted for dispersion and immobilization, we cite: (i) the electrostatic interaction of charged porphyrins with counter-charged supports; (ii) the inclusion (or intercalation) in porous (or layered) solids; and (iii) the anchoring by chemical reaction between properly functionalized porphyrins and properly functionalized supports. The materials used as supports include inorganic (molecular sieves,^{33–36} silica^{37–39} and clays^{36,39–42}) as well as organic solids (activated carbons^{43,44} and polymeric matrices like

Merryfield's resins^{8,45–50}). In all cases the physico-chemical properties of the resulting composite material may depend on the degree of dispersion of the porphyrin and on the nature of the interactions (if any) with the hosting matrix. In order to elucidate the extent of aggregation and its influence on the reactivity of the system, it is crucial to apply effective physical methods to investigate the nature of the isolated molecules and their supra-molecular species (aggregates). Most of the information on porphyrin aggregation in different solvents and matrices comes from vibrational and UV-Vis spectroscopies,^{51–54} supported by EPR in some cases. However, a detailed examination on the porphyrin aggregation and on the reactivity of the different species inside porous supports has not been published yet.

The aim of the present work is to cover this deficiency by applying very effective physical methods (FTIR, Raman, UV-Vis, and EPR spectroscopies) in the investigation of a highly dispersed cobalt(II) porphyrin encapsulated inside a high cross-linked poly(4-ethylstyrene-co-divinylbenzene) matrix. The adoption of this highly porous support, characterized by a high surface area (1000 m² g^{−1}) and a high pore volume (average diameter of 100 Å), is the key factor in reaching an optimum porphyrin dispersion. Furthermore, the presence of a permanent porous structure allows gaseous molecules to reach the Co^{II} cations, also in absence of swellable solvents. In particular, the reactivity of the isolated Co^{II} porphyrin species towards nitric oxide (NO) has been investigated. It is worth noticing that the adoption of porous polymers to disperse metal complexes has been already largely used in the past.^{55–58}

The coordination of axial ligands on metalloporphyrins is essential for the biological functionalities of these complexes and for their technical application as gas sensors and catalysts. The coordination of NO in metalloporphyrins is especially important, because NO plays a crucial role as a signalling

^a Department of Inorganic, Physical and Materials Chemistry, NIS Centre of Excellence and INSTM Centro di Riferimento, University of Turin, Via P. Giuria 7, I-10125, Torino, Italy

^b Department of General and Organic Chemistry and NIS Centre of Excellence, University of Turin, C.so M. d'Azeglio 48, I-10125, Torino, Italy

molecule in biological systems.^{59–62} Studies into the binding of NO by metalloporphyrins can help in the understanding of how NO interacts with heme-containing biomolecules, such as hemoglobin and myoglobin. Although they have not been studied as much as their iron analogs, cobalt nitrosyl porphyrins are gaining attention for the binding and activation of NO. For example, (TPP)Co(NO) has been explored as an isoelectronic model for oxygenated protoheme,⁶³ and NO adducts of Co-substituted myoglobin and hemoglobin are also known.⁶⁴ A large volume of work has been published on nitrosyl–cobaltporphyrin complexes, showing that systematic changes in porphyrin ring structure have a great influence on their chemistry and spectroscopy.^{60,63,65–69} This work well inserts in this field, offering detailed information on well isolated PhCo(NO) species by means of different complementary techniques.

2. Experimental

The solid used as support in these experiments was a commercial (Aldrich) poly(4-ethylstyrene-co-divinylbenzene) crosslinked polymer (hereafter St-DVB) characterized by a BET surface area of 920 m² g^{−1}.⁷⁰ The high surface area is actually the consequence of the presence of micropores (in the range 11–20 Å) and mesopores (20–500 Å range).

The cobalt-containing porphyrin (hereafter PhCo^{II}; see left part of Fig. 1 for the structure) was prepared by overnight refluxing a 5,10,15,20-tetrakis(4-methoxyphenyl)-21*H*,23*H*-porphine metal-free base (Sigma-Aldrich) with a stoichiometric amount of CoCl₂ using *N,N*-Dimethylformamide (puriss. p.a., for GC, > 99.9% Fluka) as solvent, according to the procedure described by Adler *et al.*⁷¹ The reaction product was purified on a SiO₂ column (Merck, 230–700 ASTM), using a CHCl₃–CH₃OH (98:2) solution as eluent. The occurrence of Co^{II} incorporation inside the free-base porphyrin ring (ring metallation) was checked by recording the UV-Vis spectra of solutions of the product in CHCl₃ (1.10^{−5} M). Ring metallation is in fact expected to cause the blue shift of the Soret band from 419 (free-base) to 412 nm (PhCo^{II}) and the red shift of the Q band from 519 (free-base) to

531 nm (PhCo^{II}). Obtained spectra were in agreement with literature data.

PhCo^{II}/St-DVB supported samples were prepared by grinding mixtures of PhCo^{II} and St-DVB (in a 1:10 weight ratio, corresponding to 1 wt% Co^{II}) in the presence of a small amount of anhydrous benzene (99.8% Aldrich) acting as solvent for the porphyrin. After drying of the solvent a red powder was obtained, suitable to be used as such for UV-Vis (diffuse reflectance), Raman and EPR experiments or to be pressed in form of self-supporting wafers for FTIR transmission experiments. Reference spectra of pure PhCo^{II} were obtained either in benzene or chloroform solutions (UV-Vis) or on a thin film supported on a silicon wafer (FTIR).

All the spectroscopic experiments were performed by using properly designed cells permanently attached to a vacuum manifold allowing *in-situ* outgassing of the samples (typically one night at room temperature to remove any trace of solvent and other adsorbed impurities) and dosage of gases.

The infrared spectra were recorded on a Bruker IFS28 Fourier Transform spectrometer (equipped with a cryogenic MCT detector) and typically correspond to the acquisition of 64 scans at 2 cm^{−1} resolution. The Raman measurements were performed on a Renishaw inVia Raman Microscope (equipped with an Olympus 20× ULWD MSPlan objective) using a 442 nm exciting line, generated by a He–Cd Kimmon laser. The choice of the 442 nm line (22 624 cm^{−1}) is justified by the fact that it falls in the Soret band of PhCo^{II}, so allowing us to obtain intensified resonance Raman spectra, as shown by Paulat *et al.*⁷² The photons scattered by the sample were dispersed by a 2400 lines/mm grating monochromator and collected on a CCD camera. The UV-Vis diffuse reflectance spectra of PhCo^{II}/St-DVB were recorded on a Perkin-Elmer Lambda-19 instrument; those of PhCo^{II} solutions on a Shimadzu UV-1700 Pharma spectrophotometer operated in transmission mode. CW-EPR spectra were collected at 77 K on a Bruker EMX spectrometer (mW frequency 9.48 GHz). The spectra were recorded at 2 mW microwave power with a modulation amplitude of 0.05 mT and a modulation frequency of 100 KHz. The simulation of the spectrum was carried out with the EPRsim 32 program.⁷³

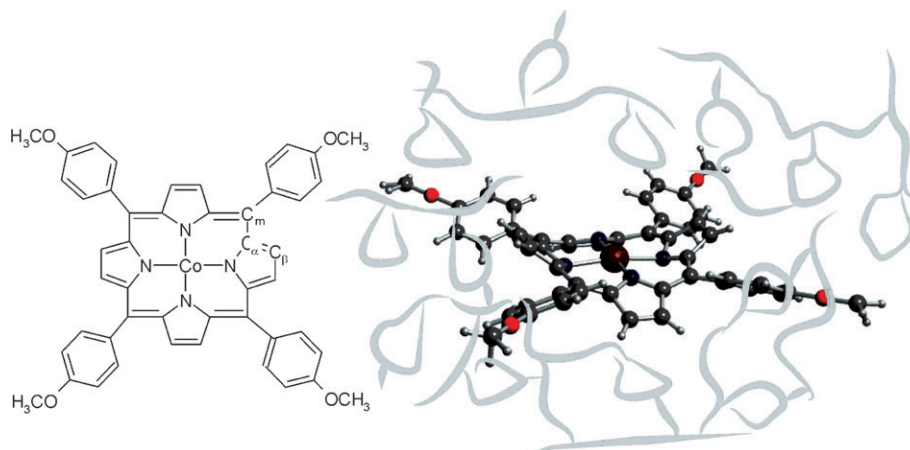


Fig. 1 Structure of the Co-porphyrin used in this work (left) and pictorial representation of a PhCo^{II} molecule encapsulated inside a St-DVB nanopore (right). In the left part the notation adopted in the assignment of the vibrational modes is also reported.

3. Results and discussion

3.1 The encapsulation of PhCo^{II} inside the St-DVB matrix: FTIR, Raman, UV-Vis and EPR study

The encapsulation of PhCo^{II} inside the St-DVB matrix (see pictorial representation in Fig. 1) has been investigated by means of complementary spectroscopic techniques.

In Fig. 2 the FTIR spectrum of the PhCo^{II} /St-DVB system (curve 2) is compared in the $1700\text{--}700\text{ cm}^{-1}$ interval with those of the pure St-DVB support (curve 1) and of the pure Co-porphyrin (curve 3). Without going into excessive details about the assignment of these spectra, which is outside the scope of this paper, we can comment the following: (i) in the St-DVB spectrum (curve 1 in Fig. 2) the bands due to the C–C stretching modes of the phenyl groups and of the polymeric chains are easily recognized in the $1650\text{--}1300\text{ cm}^{-1}$ interval. In the $1000\text{--}700\text{ cm}^{-1}$ region the CH_2 torsional modes of the chains and the out of plane C–C and C–H vibrations of the phenyl groups (see for instance ref. 74) are falling. (ii) In the spectrum of the pure PhCo^{II} porphyrin (curve 3 in Fig. 2) some characteristic absorptions can be individualized, which are related to the pyrrole units.^{75–79} In particular, we mention (see left part of Fig. 1 for the C indexing) the $\nu_s(\text{C}_\alpha\text{--N})$ stretching mode at ca. 1350 cm^{-1} , the $\nu(\text{C}_m\text{--Pyr})$ stretching at ca. 1280 cm^{-1} , the $\delta(\text{Pyr})$ bending at ca. 1250 cm^{-1} , the $\nu(\text{C}_\alpha\text{--C}_\beta)$ at ca. 1180 cm^{-1} and, finally, the $\nu_s(\text{C}_\alpha\text{--C}_m)$ stretching at ca. 990 cm^{-1} .

(iii) The spectrum of the PhCo^{II} /St-DVB system (curve 2 in Fig. 2) basically appears as the simple superposition of the features of the St-DVB matrix and of the bare PhCo^{II} molecule (except for the fact that the band due to the $\delta(\text{Pyr})$ bending appears as a doublet at 1248 and 1238 cm^{-1} in the pure porphyrin and as a singlet at 1248 cm^{-1} in the mixed system). The absence of any significant modifications in the spectra of the matrix and of the porphyrin when mixed to give the PhCo^{II} /St-DVB system could be of course interpreted as a lack of intimate mixing between the two precursors and hence as a sign of failure of the porphyrin to diffuse inside the internal voids of the polymeric matrix. As it will be shown

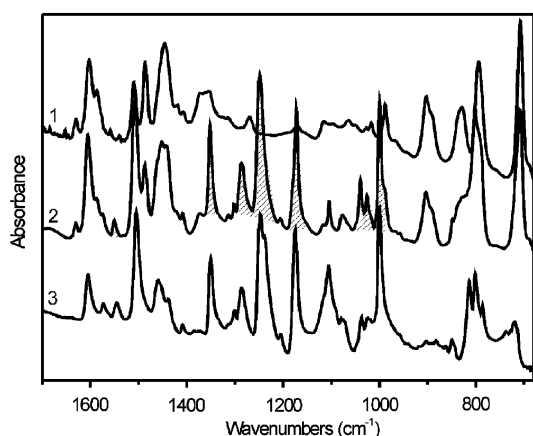


Fig. 2 FTIR spectra of (1) pure St-DVB, (2) PhCo^{II} /St-DVB, and (3) pure PhCo^{II} . All the spectra were obtained after prolonged outgassing of the samples at room temperature under high vacuum ($<10^{-6}$ mbar). The shaded portions of the PhCo^{II} /St-DVB spectrum (curve 2) indicate the bands characteristic of the entrapped PhCo^{II} species.

in the following, this is not actually the case: in fact, the Raman and UV-Vis experiments clearly demonstrate that PhCo^{II} is encapsulated inside the St-DVB micropores and dispersed down to the molecular level. On this basis, the results of Fig. 2 seem rather to suggest the lack of any interaction between the matrix and the entrapped molecules, which could possibly involve the aromatic rings of St-DVB and the Co^{II} centres. This kind of “lateral” interactions are on the contrary quite usual in homogeneous conditions:^{3,4,80} we can therefore conclude that the polymeric matrix acts as a non-coordinating solvent.

The FTIR spectrum of the PhCo^{II} /St-DVB system in the $1700\text{--}700\text{ cm}^{-1}$ range (curve 2 in Fig. 2) gives information only on the skeletal modes of the entrapped porphyrin ring, *i.e.* on vibrations which are only little or negligibly sensitive to the presence of the metal centre and to its coordination state. Furthermore, the direct observation of those modes involving the metal centre, like the $\nu(\text{Co--N})$ breathing vibration, which are expected to fall at wavenumbers definitely lower than 500 cm^{-1} ,^{72,77} is prevented for experimental reasons. Raman spectroscopy easily allows us to overcome the FTIR frequency limitations. Furthermore, when operated in resonance conditions (*i.e.* by using an exciting line matching one of the allowed electronic transition of the porphyrin) the M-Pyr vibrations (where M represent the metal centre and Pyr the Pyrrole units) are selectively enhanced in intensity and become particularly intense.⁷²

The resonance enhanced Raman spectrum of the PhCo^{II} /St-DVB system, as obtained using a 442 nm (22624 cm^{-1}) excitation line, falling in the PhCo^{II} Soret band (*vide infra*), is reported in Fig. 3 (black curve). Beside the bands in the $1700\text{--}700\text{ cm}^{-1}$, due to the organic structure surrounding the Co^{II} centre (which are similar to those already discussed above in the FTIR section), it is noticeable the presence of a very intense peak at 380 cm^{-1} (inset in Fig. 3) which, in agreement with Paulat *et al.*⁷² (who have studied the normal and resonance

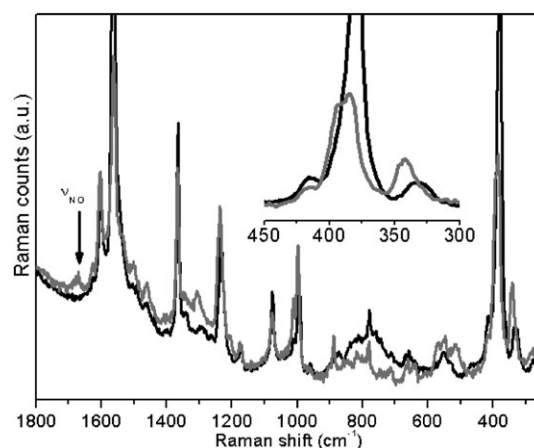


Fig. 3 Raman spectra of PhCo^{II} /St-DVB before (black) and after (gray) interaction with NO ($P_{\text{NO}} = 10\text{ mbar}$) at RT. The inset illustrates in greater detail the $450\text{--}300\text{ cm}^{-1}$ region typical of the $\nu(\text{Co--N})$ breathing modes of the porphyrin core. The arrow indicates the weak band assigned to the stretching mode of coordinated NO. The spectra were obtained in resonance conditions, using the 442 nm (22624 cm^{-1}) exciting laser line matching the Soret electronic transition of PhCo^{II} .

enhanced Raman spectra of a variety of metal porphyrins molecularly dispersed in KBr matrices) can be readily assigned to the $\nu(\text{Co}-\text{N})$ breathing mode of the porphyrin core.

The solid state UV-Vis spectrum of the $\text{PhCo}^{\text{II}}/\text{St-DVB}$ system is compared in Fig. 4 (black curve) with that of the pure St-DVB matrix (dotted curve) and with those of the pure PhCo^{II} porphyrin in two different solvents (benzene and chloroform, light and dark grey curves, respectively). In both the solvents the pure porphyrin shows absorption bands centred at $24\,200\text{ cm}^{-1}$ (410 nm, very strong), $19\,000\text{ cm}^{-1}$ (525 nm, medium) and $16\,200\text{ cm}^{-1}$ (615 nm, weak). These absorptions are thoroughly discussed in specialized literature concerning the optical properties of porphyrins and phthalocyanines,^{52,65,81–83} and referred to as Soret ($24\,200\text{ cm}^{-1}$) and Q bands ($19\,000$ and $16\,200\text{ cm}^{-1}$). The Soret band is electronically allowed and is one order of magnitude more intense than the Q-band. Beside the above bands, which are originated by transitions mainly involving the electronic levels of the organic part of the PhCo^{II} molecule, in the $14\,000\text{--}10\,000\text{ cm}^{-1}$ interval (see inset in Fig. 4) the spectra also show a very weak (and possibly complex) band, which is assigned to the $^2\text{B}_2 \rightarrow ^2\text{E}_g$ d–d transition of the low-spin Co^{II} cation in a square-planar geometry.^{84–86} The broadness of this bands (which in the case of PhCo^{II} in benzene solution is clearly split in two components, at $11\,900$ and $11\,200\text{ cm}^{-1}$) is an indication of structural heterogeneity and is due to the existence even in diluted solution of very small $[\text{PhCo}^{\text{II}}]_n$ clusters (like dimers, trimers, *etc.*).

The optical spectrum of the $\text{PhCo}^{\text{II}}/\text{St-DVB}$ system (full black curve in Fig. 4) is very similar to those of PhCo^{II} in benzene or chloroform solution as far as the band width and the position of the Soret and Q bands are concerned (the main difference being represented by a moderate red-shift of the

Soret band to $23\,500\text{ cm}^{-1}$, 425 nm).[†] It is worth underlining in this respect that for porphyrins intercalation in clays or encapsulation in the cavities of zeolitic materials significant broadening and shift of the electronic absorptions are observed as compared to the same molecules in solutions.^{34,36} This is an indication that the above matrices interact with the hosted porphyrin molecules, so affecting their electronic properties. The absence of similar effects in the case of the $\text{PhCo}^{\text{II}}/\text{St-DVB}$ system reinforces the view that the polymeric matrix is acting as an “inert solvent”.

As far as the d–d transition region is concerned ($14\,000\text{--}10\,000\text{ cm}^{-1}$, see the inset in Fig. 4) the differences between the spectrum of PhCo^{II} in St-DVB and those of the porphyrin in benzene or chloroform solutions appear remarkable: the broad band observed for $\text{PhCo}^{\text{II}}/\text{CHCl}_3$ or the doublet observed for $\text{PhCo}^{\text{II}}/\text{C}_6\text{H}_6$, in fact, is now resolved in a very narrow absorption at $11\,300\text{ cm}^{-1}$, accompanied by three weaker bands at $13\,000$, $12\,200$ and $10\,500\text{ cm}^{-1}$. The very regular spacing between the components of this quadruplet (*ca.* 800 cm^{-1}) suggests that it could be likely due to vibronic coupling effects. The vibronic structure is absent (or nearly absent) in solution, because of the tendency to clustering of the porphyrin molecules (with formation of dimers, trimers, *etc.*) and/or the axial interaction between the Co^{II} centres and the molecules of the solvent. The appearance of the vibronic structure in the $\text{PhCo}^{\text{II}}/\text{St-DVB}$ system is therefore a direct proof of the molecular dispersion of the Co-porphyrin encapsulated inside the St-DVB voids. To the best of our knowledge, this is the first time that such a fine structure has been reported in the optical spectra of square-planar Co^{II} complexes.

In order to further confirm the hypothesis advanced above about the molecular dispersion of the porphyrin and the absence of strong interaction with the St-DVB scaffold (possibly through axial interaction of the Co^{II} centres with the dangling phenyl rings), EPR experiments have been carried out. It is, in fact, well-known that the EPR spectra of low-spin planar Co^{II} complexes, and among them especially those of phthalocyanines and porphyrins, are characterized by extreme sensitivity to solvation or axial interactions with coordinating ligands.^{84,87–93} This sensitivity arises from the d_{22} configuration of the unpaired spin, which has its maximum density along the axial directions.

The CW EPR spectrum of the $\text{PhCo}^{\text{II}}/\text{St-DVB}$ sample recorded at 77 K is shown in Fig. 5a. The spin Hamiltonian for a low spin Co^{II} system (electron configuration $3d^7$, $S = 1/2$, $I = 7/2$) is given by: $H = \beta \mathbf{B}_0 \mathbf{g} \mathbf{S} + \mathbf{S} \mathbf{A}^{\text{Co}} \mathbf{I}$, where the first term is the electron Zeeman interaction and the second represents the hyperfine interaction of the unpaired electron with the cobalt nucleus. These are the terms which largely dominates in the X band CW EPR spectrum reported in Fig. 5a, which is characterized by an axial g matrix and a distinct eight line hyperfine pattern due to the hyperfine interaction of the unpaired electron with the Co nucleus

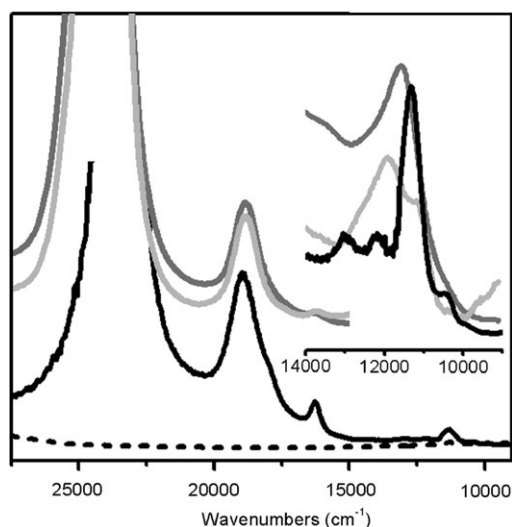


Fig. 4 Full black line: UV-Vis diffuse reflectance spectrum of $\text{PhCo}^{\text{II}}/\text{St-DVB}$. Dashed black line: UV-Vis diffuse reflectance spectrum of pure St-DVB. Full light-gray line: transmission UV-Vis spectrum of pure PhCo^{II} in benzene solution. Full dark-grey line: transmission UV-Vis spectrum of pure PhCo^{II} in chloroform solution. The spectra of PhCo^{II} solutions are vertically translated for clarity. The inset shows a magnification ($\times 20$) of the $14\,000\text{--}9\,000\text{ cm}^{-1}$ region, typical of the Co^{II} d–d transitions.

[†] Note that the relative intensity between the Soret and Q bands in the spectra of $\text{PhCo}^{\text{II}}/\text{PS}$ is slightly different with respect to that observed for the same complex in solution due to the different acquisition mode, *i.e.* reflectance *vs.* transmission, respectively.

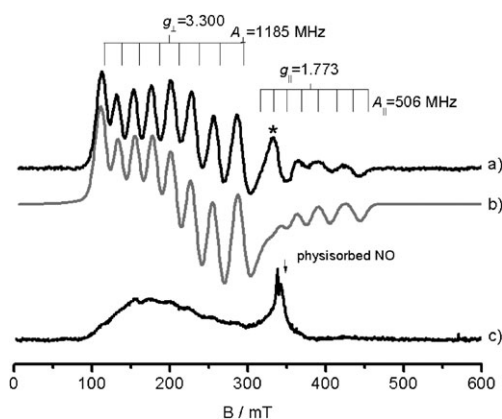


Fig. 5 Experimental (a) and computer simulated (b) EPR spectra of the $\text{PhCo}^{\text{II}}/\text{St-DVB}$ system collected at 77 K. Curve (c) is the spectrum resulting after prolonged contact of the $\text{PhCo}^{\text{II}}/\text{St-DVB}$ system with NO ($P_{\text{NO}} = 10$ mbar) at 77 K. The asterisk indicates an impurity signal which is not accounted for in the simulation.

($I = 7/2$). Computer simulation of the spectrum (see Fig. 5b) allows to determine the relevant spin Hamiltonian parameters, which are reported in Table 1 along with those of other Co^{II} porphyrin systems.

In a first order approximation, the ground state of an axial low-spin d^7 Co^{II} porphyrin can be written as $(d_{xz})^2(d_{yz})^2(d_{xy})^2(d_{z^2})^1$, whereby the coordinate system is chosen so that the x and y direction coincide with the Co–N directions in the porphyrin plane. The principal value g_{\perp} depends mainly on the energy difference $\Delta E(d_{xz,yz} \rightarrow d_{z^2})$ between the d_{z^2} and the $d_{xz,yz}$ orbitals and can be approximated by:^{88,89,94,95} $g_{\perp} = 2.0023 + \lambda/\Delta E(d_{xz,yz} \rightarrow d_{z^2})$, where $\lambda = 515 \text{ cm}^{-1}$ is the spin–orbit coupling constant of Co^{II} . The value of ΔE depends on the strength of the axial field: the stronger the axial perturbation, the larger the energy difference and the more the g_{\perp} value will be close to 2.0023. In the same way the cobalt hyperfine values are related to the axial perturbation introduced by the presence of axial ligands. In particular, the larger the axial perturbation the smaller the g_{\perp} , A_{\perp} and A_{\parallel} values. For the lowest possible axial field, g_{\perp} approaches values in the range 3.2–3.4, while g_{\parallel} tends to be relatively close to 2.0. It can therefore be concluded that the

magnetic anisotropy $g_{\parallel}^2 - g_{\perp}^2$ for a given porphyrin complex is a reasonable index of the strength of the axial field.

Examination of Table 1 indicates that the spin Hamiltonian parameters for $\text{PhCo}^{\text{II}}/\text{St-DVB}$ are in good agreement with those reported for $\text{Co}(\text{p-OCH}_3)\text{TPP}$ and similar Co^{II} containing porphyrins diluted in diamagnetic host porphyrins or intercalated in clays,⁴¹ and completely different from those observed in the case of Co^{II} porphyrins in different solvents.^{84,87–92} It should be noted that Co^{II} porphyrins form charge transfer (CT) complexes with strong π acceptors (such as H_2TPP), which bring about a rearrangement of the metal d orbitals leading to small ΔE values and consequently high g_{\perp} factors. In our system, however, we can exclude the presence of such π acceptor systems and thus we can take the spin Hamiltonian parameters reported in Table 1 as an evidence of the fact the Co porphyrins are isolated and unperturbed. In particular, the EPR spectrum can be interpreted in terms of negligible axial interactions, as already reported in the case of Co^{II} porphyrins highly diluted in the corresponding Co-free bases^{89,96} and in clays.⁴¹

By combining the FTIR, Raman, UV-Vis and EPR results, we can therefore finally conclude that PhCo^{II} is molecularly encapsulated inside the micro-cavities of the St-DVB matrix without evidence of any axial interaction, as pictorially represented in the right part of Fig. 1. This is an even more noticeable result when taking into consideration that in the present work we are dealing with rather concentrated samples. This molecularly dispersed system is an ideal model to investigate the interaction of PhCo^{II} with NO.

3.2 The interaction of the $\text{PhCo}^{\text{II}}/\text{St-DVB}$ system with NO

Dosage of NO on $\text{PhCo}^{\text{II}}/\text{St-DVB}$ induces a slow but dramatic modification of the EPR spectrum (Fig. 5c), consisting in the complete disappearance of the previously observed hyperfine structure. This behaviour suggests the formation of PhCo^{II} –nitrosyl complexes characterized by different structural and electronic properties with respect to the precursor porphyrin. In particular, as the NO ligand possess an unpaired electron in a π^* orbital, formation of the nitrosyl complex implies coupling with the unpaired d_{z^2} electron of PhCo^{II} and hence the disappearance of the Co^{II} EPR signal.

Table 1 Spin Hamiltonian parameters for different Co^{II} porphyrins

g_{\perp}	$g_{ }$	A_{\perp} /MHz	$A_{ }$ /MHz	$g_{ }^2-g_{\perp}^2$	Ref.	
Co(p-OCH ₃)TPP						
PS	3.300	1.773	1185	506	−7.7	This work
In Ni(p-OCH ₃)TPP	3.317	1.75	1208	585	−7.9	89
In H ₂ (p-OCH ₃)TPP	3.264	1.81	1121	513	−7.4	89
In toluene	2.848	2.006	683	483	−4.1	89
Co(p-CH ₃)TPP						
In H ₂ (p-CH ₃)TPP	3.193	1.84	1056	519	−6.8	89
In toluene	2.97	1.966	816	414	−4.9	89
CoTPP						
In NiTPP	3.35	1.73	1245	542	−8.2	96
In ZnTPP	3.3	1.75	1190	518	−7.8	96
In toluene (1 : 1)	2.75	1.95	612	416	−3.8	92, 96
CoTMPyP						
In hectorite	3.1045	1.8570	974	438	−6.2	41
In H ₂ O solution	2.4406	2.0258	174	300	−1.8	41

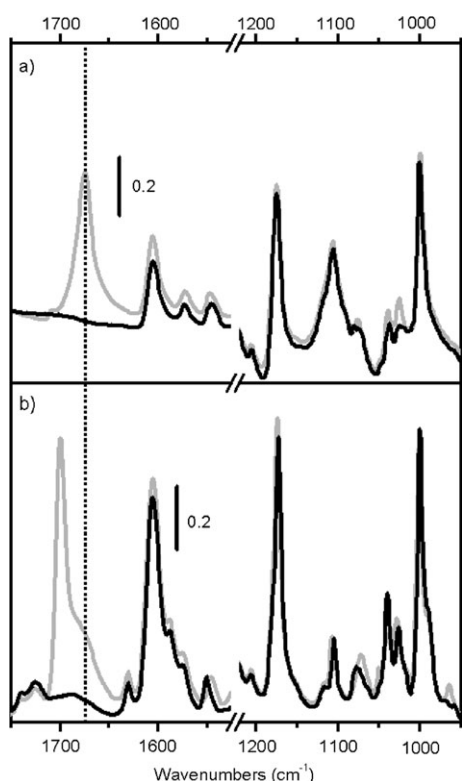


Fig. 6 FTIR spectra of PhCo^{II} (thin film on silicon) (part a) and of $\text{PhCo}^{\text{II}}/\text{St-DVB}$ (part b), before (black curves) and after (grey curves) NO adsorption ($P_{\text{NO}} = 10$ mbar). The position of the $\nu(\text{NO})$ band due to the nitrosylic species formed on pure PhCo^{II} in solid state is marked for reference by the vertical dotted line.

In order to better characterize the nitrosylic species responsible for the EPR changes discussed above, the adsorption of NO on $\text{PhCo}^{\text{II}}/\text{St-DVB}$, and on pure PhCo^{II} , has been also studied by FTIR, Raman and UV-Vis spectroscopies. Starting with FTIR spectroscopy, when NO ($P_{\text{NO}} = 10$ Torr) is dosed at RT on pure PhCo^{II} (in solid state as thin film deposited on silicon) a new rather intense absorption immediately appears in the nitrosylic region of the FTIR spectrum at 1674 cm^{-1} (gray curve in Fig. 6a). The observed $\tilde{\nu}(\text{NO})$ is close to that reported in previous studies for adducts formed on the same Co-porphyrin dispersed in KBr (1679 cm^{-1}) or in solution (1682 cm^{-1} in CH_2Cl_2)⁶⁶ as well as for nitrosylic complexes formed on structurally different systems, like (TPP)Co(NO) (1689 cm^{-1} in KBr)^{63,65} or (OEP)Co(NO) (1675 cm^{-1} in CH_2Cl_2); similar $\tilde{\nu}(\text{NO})$ values ($1645\text{--}1675\text{ cm}^{-1}$) are also observed for square pyramidal *N*-substituted Co-salicylideaminates, where the NO ligand is known to assume a bent configuration.⁹⁷ Bent NO structures (with M–N–O angles in the $120\text{--}135^\circ$ range) are also typical of $\{\text{M}(\text{NO})\}_8^+$ nitrosyl metalloporphyrin homologues, where the metal centre is placed out of the porphyrin plane in a local square-pyramidal configuration.^{63,65,68} Characteristic of bent NO complexes is the fairly large downward shift of $\tilde{\nu}(\text{NO})$ frequency (about -200 cm^{-1} , *i.e.* similar to that observed in the present case) with respect to gaseous NO (1876 cm^{-1}), which is often interpreted on the basis of formation of negatively charged $(\text{NO})^{\delta-}$ species.^{63,65,68} Linear nitrosyls, sometimes considered

consistent with formation of positively charged $(\text{NO})^{\delta+}$ species, give rise to smaller downward shifts. Coordination of NO on the metal centre has almost no influence on the vibrational manifestations of the organic part of the porphyrin, except for the growth of two weak bands at 1075 and 1024 cm^{-1} .

In conclusion of this part we underline that, as the reaction of PhCo with NO to give bent $\text{PhCo}(\text{NO})$ nitrosylic species is occurring in the solid state, the product molecules cannot be considered as “isolated”, but in strong interaction with each other. This allows us to consider the $\tilde{\nu}(\text{NO})$ peak at 1674 cm^{-1} as a fingerprint of $[\text{PhCo}(\text{NO})]_n$ clustered species.

As compared to the pure porphyrin (*vide supra*), the modifications of the IR spectrum of the $\text{PhCo}^{\text{II}}/\text{St-DVB}$ system upon NO adsorption are more pronounced (Fig. 6b). In fact, two well-defined components appear immediately in the $\tilde{\nu}(\text{NO})$ region, one more intense and sharp, centred at 1700 cm^{-1} , and a second broader one centred at the same frequency observed for the $[\text{PhCo}(\text{NO})]_n$ film. Based on the conclusions advanced in the previous paragraph, that the porphyrin molecules are encapsulated in the St-DVB matrix in a highly dispersed form, we assign the strong 1700 cm^{-1} peak to the $\tilde{\nu}(\text{NO})$ stretching mode of “isolated” $\text{PhCo}(\text{NO})$ species dispersed in the St-DVB matrix, whereas the weaker component at 1674 cm^{-1} is assigned to a small fraction of residual clustered species possibly formed on the external surface of the polymeric particles and/or in the large St-DVB macro-pores. As the NO extinction coefficient is expected to not change significantly on passing from the isolated to the clustered species (because of the small differences in frequency), the much higher intensity of the 1700 cm^{-1} peak is a direct evidence that highly dispersed $\text{PhCo}(\text{NO})$ species are predominant. Also in this case, the NO coordination does not substantially affect the FTIR spectrum in the region of the vibrational modes of the organic structure surrounding the metal centre.

The coordination of NO to the metal centre is, on the contrary, expected to selectively perturb the $\nu(\text{Co-N})$ core vibrations actually observed at *ca.* 390 cm^{-1} (see black curve in Fig. 3). That this is the case is demonstrated by the Raman spectrum obtained after NO dosage and reported in Fig. 3 (grey curve). From the comparison of the spectra obtained before and after NO dosage it can be commented and concluded that: (a) the weak peak observed at *ca.* 1780 cm^{-1} is certainly due to the $\nu(\text{NO})$ mode of coordinated NO in the $\text{PhCo}(\text{NO})$ adducts. The weakness of the Raman manifestation is not surprising when considering the high intensity observed for the same species in the IR. (b) The modes at frequency higher than 500 cm^{-1} are substantially unaffected (as expected, being due to the organic part of the porphyrin). (c) The band at 380 cm^{-1} , due to the $\tilde{\nu}(\text{Co-N})$ breathing mode, is shifted to higher frequency (at 390 cm^{-1}) (inset in Fig. 3). The upward shift confirms that the formed complex can be considered as a $\text{PhCo}^{\text{III}}(\text{NO})$ species, as it is known that the breathing mode shifts to higher frequencies upon increasing the charge on the metal centre.⁷²

Nitrosyl complex formation in the $\text{PhCo}^{\text{II}}/\text{St-DVB}$ sample causes relevant changes not only in the structural but also in the electronic properties of the porphyrin, as testified by

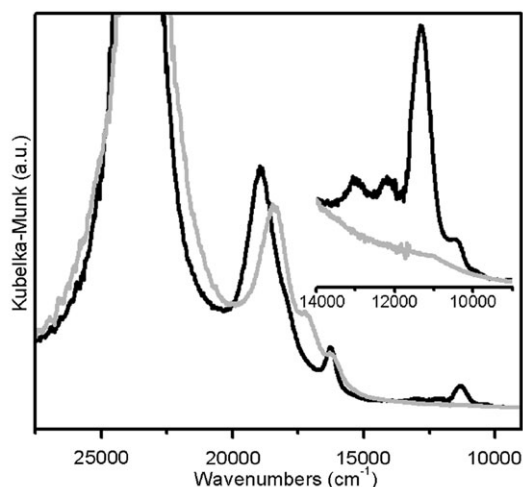


Fig. 7 Optical changes in the UV-Vis spectrum of the PhCo^{II} /St-DVB sample (black curve) upon NO adsorption (grey curve, $P_{\text{NO}} = 10$ mbar). The inset reports a magnification of the 14000–9000 cm^{-1} d–d transition region.

UV-Vis spectroscopy (grey curve in Fig. 7). In particular, in the high frequency region: (a) the Soret band slightly shifts towards lower frequencies; (b) the Q bands shift to lower frequencies and split in several components. Similar spectral modifications were observed upon NO adsorption on Co^{II} TPP systems in toluene solutions.⁶⁵ In the d–d transition region (inset in Fig. 7), adsorption of NO causes the disappearance of the spin–orbit quartet associated with $^2\text{B}_2 \rightarrow ^2\text{E}_g$ transition. This drastic modification is in agreement with the increase in coordination of the Co^{II} center caused by NO coordination. In this respect, it is a matter of fact that the extinction coefficient of the Co^{II} d–d transitions is known to decrease about 100 times on passing from tetrahedral to octahedral complexes.⁹⁸

4. Conclusions

This work demonstrates that the St-DVB internal pores can act as nano-scaffolds for entrapping PhCo^{II} , so allowing its dispersion down to the molecular level, as pictorially represented in Fig. 1. The entrapped PhCo^{II} species, investigated by means of FTIR, Raman, UV-Vis and EPR spectroscopies, are characterized by the absence of any axial interactions involving the dangling phenyl rings of the polymeric matrix and the porphyrin metal centres (which are on the contrary quite common in homogeneous conditions, where the solvent molecules easily enter the Co^{II} coordination sphere): St-DVB can be therefore considered as a “non-coordinating” solid solvent. Furthermore, the permanent porous structure of the polymeric matrix allows gaseous molecules to reach the Co^{II} centers, also in absence of swellable solvents and the spectroscopic properties of the Co^{II} -nitrosil species formed upon dosing NO have been investigated.

References

- 1 D. Mansuy, *C. R. Chim.*, 2007, **10**, 392.
- 2 M. Wolak and R. van Eldik, *Chem.–Eur. J.*, 2007, **13**, 4873.

- 3 R. Naik, P. Joshi and R. K. Deshpande, *J. Mol. Catal. A: Chem.*, 2005, **238**, 46.
- 4 R. Naik, P. Joshi, S. Umbarkar and R. K. Deshpande, *Catal. Commun.*, 2005, **6**, 125.
- 5 M. Hassanein, S. Gerges, M. Abdo and S. El-Khalafy, *J. Mol. Catal. A: Chem.*, 2005, **240**, 22.
- 6 G. Mele, R. Del Sole, G. Vasapollo, E. Garcia-Lopez, L. Palmisano and M. Schiavello, *J. Catal.*, 2003, **217**, 334.
- 7 V. Maraval, J. E. Ancel and B. Meunier, *J. Catal.*, 2002, **206**, 349.
- 8 A. Maldotti, L. Andreotti, A. Molinari, S. Borisov and V. Vasil'ev, *Chem.–Eur. J.*, 2001, **7**, 3564.
- 9 N. A. Stephenson and A. T. Bell, *J. Mol. Catal. A: Chem.*, 2007, **275**, 54.
- 10 E. Rose, B. Andrioletti, S. Zrig and M. Quelquejeu-Ehteve, *Chem. Soc. Rev.*, 2005, **34**, 573.
- 11 B. Meunier, S. P. de Visser and S. Shaik, *Chem. Rev.*, 2004, **104**, 3947.
- 12 A. Maldotti, C. Bartocci, G. Varani, A. Molinari, P. Battioni and D. Mansuy, *Inorg. Chem.*, 1996, **35**, 1126.
- 13 T. G. Traylor, C. Kim, J. L. Richards, F. Xu and C. L. Perrin, *J. Am. Chem. Soc.*, 1995, **117**, 3468.
- 14 G. D. Silva, D. C. da Silva, A. S. Guimaraes, E. do Nascimento, J. S. Reboucas, M. P. de Araujo, M. de Carvalho and Y. M. Idemori, *J. Mol. Catal. A: Chem.*, 2007, **266**, 274.
- 15 Z. L. Fang and R. Breslow, *Org. Lett.*, 2006, **8**, 251.
- 16 H. S. He, B. S. Fang, J. W. Huang and L. N. Ji, *Transition Met. Chem.*, 2000, **25**, 352.
- 17 J. W. Huang, Z. L. Liu, X. R. Gao, D. Yang, X. Y. Peng and L. N. Ji, *J. Mol. Catal. A: Chem.*, 1996, **111**, 261.
- 18 N. Hessenauer-Ilicheva, A. Franke, D. Meyer, W. D. Woggon and R. van Eldik, *J. Am. Chem. Soc.*, 2007, **129**, 12473.
- 19 A. Franke, N. Hessenauer-Ilicheva, D. Meyer, G. Stochel, W. D. Woggon and R. van Eldik, *J. Am. Chem. Soc.*, 2006, **128**, 13611.
- 20 I. G. Denisov, T. M. Makris, S. G. Sligar and I. Schlichting, *Chem. Rev.*, 2005, **105**, 2253.
- 21 J. P. Collman, A. S. Chien, T. A. Eberspacher and J. I. Brauman, *J. Am. Chem. Soc.*, 2000, **122**, 11098.
- 22 A. Gonsalves and M. M. Pereira, *J. Mol. Catal. A: Chem.*, 1996, **113**, 209.
- 23 B. Meunier, *Chem. Rev.*, 1992, **92**, 1411.
- 24 M. J. Gunter and P. Turner, *Coord. Chem. Rev.*, 1991, **108**, 115.
- 25 R. Paolesse, D. Monti, L. La Monica, M. Venanzi, A. Froio, S. Nardis, C. Di Natale, E. Martinelli and A. D'Amico, *Chem.–Eur. J.*, 2002, **8**, 2476.
- 26 A. D'Amico, C. Di Natale, R. Paolesse, A. Macagnano and A. Mantini, *Sens. Actuators, B*, 2000, **65**, 209.
- 27 D. Delmarre and C. Bied-Charreton, *Sens. Actuators, B*, 2000, **62**, 136.
- 28 H. L. Anderson, *Chem. Commun.*, 1999, 2323.
- 29 I. Leray, M. C. Vernieres, R. LoucifSaïbi, C. BiedCharreton and J. Faure, *Sens. Actuators, B*, 1996, **37**, 67.
- 30 Q. Wang, W. M. Campbell, E. E. Bonfantani, K. W. Jolley, D. L. Officer, P. J. Walsh, K. Gordon, R. Humphry-Baker, M. K. Nazeeruddin and M. Gratzel, *J. Phys. Chem. B*, 2005, **109**, 15397.
- 31 W. M. Campbell, A. K. Burrell, D. L. Officer and K. W. Jolley, *Coord. Chem. Rev.*, 2004, **248**, 1363.
- 32 D. Wohrle and D. Meissner, *Adv. Mater.*, 1991, **3**, 129.
- 33 J. L. Zhang, Y. L. Liu and C. M. Che, *Chem. Commun.*, 2002, 2906.
- 34 B. T. Holland, C. Walkup and A. Stein, *J. Phys. Chem. B*, 1998, **102**, 4301.
- 35 H. M. SungSuh, Z. H. Luan and L. Kevan, *J. Phys. Chem. B*, 1997, **101**, 10455.
- 36 F. Bedioui, *Coord. Chem. Rev.*, 1995, **144**, 39.
- 37 A. D. Q. Ferreira, F. S. Vinhado and Y. Iamamoto, *J. Mol. Catal. A: Chem.*, 2006, **243**, 111.
- 38 M. S. M. Moreira, P. R. Martins, R. B. Curi, O. R. Nascimento and Y. Iamamoto, *J. Mol. Catal. A: Chem.*, 2005, **233**, 73.
- 39 M. A. MartinezLorente, P. Battioni, W. Kleemiss, J. F. Bartoli and D. Mansuy, *J. Mol. Catal. A: Chem.*, 1996, **113**, 343.
- 40 S. Takagi, T. Shimada, M. Eguchi, T. Yui, H. Yoshida, D. A. Tryk and H. Inoue, *Langmuir*, 2002, **18**, 2265.

- 41 L. Ukrainczyk, M. Chibwe, T. J. Pinnavaia and S. A. Boyd, *J. Phys. Chem.*, 1994, **98**, 2668.
- 42 M. Onaka, T. Shinoda, Y. Izumi and E. Nolen, *Chem. Lett.*, 1993, 117.
- 43 I. T. Bae, D. A. Tryk and D. A. Scherson, *J. Phys. Chem. B*, 1998, **102**, 4114.
- 44 R. F. Parton, P. E. Neys, P. A. Jacobs, R. C. Sosa and P. G. Rouxhet, *J. Catal.*, 1996, **164**, 341.
- 45 S. M. Ribeiro, A. C. Serra and A. Gonsalves, *Tetrahedron*, 2007, **63**, 7885.
- 46 E. Burri, M. Ohm, C. Daguene and K. Severin, *Chem.-Eur. J.*, 2005, **11**, 5055.
- 47 O. Nestler and K. Severin, *Org. Lett.*, 2001, **3**, 3907.
- 48 M. V. Vinodu and M. Padmanabhan, *J. Polym. Sci. Pol. Chem.*, 2001, **39**, 326.
- 49 T. Mathew and S. Kuriakose, *J. Porphyrins Phthalocyanines*, 1999, **3**, 316.
- 50 T. Mathew, M. Padmanabhan and S. Kuraikose, *J. Appl. Polym. Sci.*, 1996, **59**, 23.
- 51 R. F. Pasternack, P. R. Huber, P. Boyd, G. Engasser, L. Francesconi, E. Gibbs, P. Fasella, G. Cerio Venturo and L. d. Hindsz, *J. Am. Chem. Soc.*, 1972, **94**, 4511.
- 52 E. S. Dodsworth, A. B. P. Lever, P. Seymour and C. C. Leznoff, *J. Phys. Chem.*, 1985.
- 53 X. M. Guo, C. Jiang and T. S. Shi, *Inorg. Chem.*, 2007, **46**, 4766.
- 54 J. Mosinger, M. Janoskova, K. Lang and P. Kubat, *J. Photochem. Photobiol., A*, 2006, **181**, 283.
- 55 L. D. Rollmann, *J. Am. Chem. Soc.*, 1975, **97**, 2132.
- 56 B. M. L. Diosa, I. F. J. Vankelecom and P. A. Jacobs, *Adv. Synth. Catal.*, 2006, **348**, 1413.
- 57 P. Hodge, *Chem. Soc. Rev.*, 1997, **26**, 417.
- 58 P. Barbaro, *Chem.-Eur. J.*, 2006, **12**, 5666.
- 59 M. D. Lim, I. M. Lorkovic and P. C. Ford, *J. Inorg. Biochem.*, 2005, **99**, 151.
- 60 P. C. Ford, J. Bourassa, K. Miranda, B. Lee, I. Lorkovic, S. Boggs, S. Kudo and L. Laverman, *Coord. Chem. Rev.*, 1998, **171**, 185.
- 61 S. Moncada, R. M. J. Palmer and E. A. Higgs, *Pharmacol. Rev.*, 1991, **43**, 109.
- 62 L. J. Ignarro, *Annu. Rev. Pharmacol. Toxicol.*, 1990, **30**, 535.
- 63 W. R. Scheidt and J. L. Hoard, *J. Am. Chem. Soc.*, 1973, **95**, 8281.
- 64 H. Hori, M. Ikeda-Saito, J. S. Leigh, Jr and T. Yonetani, *Biochemistry*, 1982, **21**, 1431.
- 65 B. B. Wayland, J. V. Minkiewicz and M. E. Abd-Elmageed, *J. Am. Chem. Soc.*, 1974, **96**, 2795.
- 66 G. B. Richter-Addo, S. J. Hodge, G. B. Yi, M. A. Khan, T. Ma, E. VanCaemelbecke, N. Guo and K. M. Kadish, *Inorg. Chem.*, 1996, **35**, 6530.
- 67 M. K. Ellison and W. R. Scheidt, *Inorg. Chem.*, 1998, **37**, 382.
- 68 G. R. A. Wyllie and W. R. Scheidt, *Chem. Rev.*, 2002, **102**, 1067.
- 69 M. Jaworska, *Chem. Phys. Lett.*, 2007, **332**, 203.
- 70 G. Spoto, J. G. Vitillo, D. Cocina, A. Damin, F. Bonino and A. Zecchina, *Phys. Chem. Chem. Phys.*, 2007, **9**, 4992.
- 71 A. Adler, F. Longo, F. Kampas and J. Kim, *J. Inorg. Nucl. Chem.*, 1970, **32**, 2443.
- 72 F. Paulat, V. K. K. Praneeth, C. Nather and N. Lehnert, *Inorg. Chem.*, 2006, **45**, 2835.
- 73 T. Spalek, P. Pietrzyk and Z. Sojka, *J. Chem. Inf. Model.*, 2005, **45**, 18.
- 74 F. J. Torres, B. Civalieri, C. Pisani, P. Musto, A. R. Albulnia and G. Guerra, *J. Phys. Chem. B*, 2007, **111**, 6327.
- 75 K. Nakamoto, *Infrared and Raman Spectra of Inorganic and Coordination Compounds*, John Wiley & Sons, New York, 1978.
- 76 D. Dolphin, in *The Porphyrins*, Academic Press, London, 1978, vol. 3.
- 77 N. Blom, J. Odo, K. Nakamoto and D. P. Strommen, *J. Phys. Chem.*, 1986, **90**, 2847.
- 78 X.-Y. Li, R. S. Czernuszewicz, J. R. Kincaid, Y. O. Su and T. J. Spiro, *J. Phys. Chem.*, 1990, **94**, 31.
- 79 X.-Y. Li and M. Z. Zgierski, *J. Phys. Chem.*, 1991, **95**, 4268.
- 80 H. J. Schneider and M. Wang, *J. Org. Chem.*, 1994, **59**, 7464.
- 81 G. D. Dorough, J. R. Miller and F. M. Huennekens, *J. Am. Chem. Soc.*, 1951, **73**, 4315.
- 82 M. Gouterman, *J. Mol. Spectrosc.*, 1961, **6**, 138.
- 83 L. Edwards, D. H. Dolphin, M. Gouterman and A. D. Adler, *J. Mol. Spectrosc.*, 1971, **38**, 16.
- 84 Y. Nishida and S. Kida, *Coord. Chem. Rev.*, 1979, **27**, 275.
- 85 B. S. Jaynes, L. H. Doerrer, S. C. Liu and S. J. Lippard, *Inorg. Chem.*, 1995, **34**, 5735.
- 86 S. A. Carabineiro, L. C. Silva, P. T. Gomes, L. C. J. Pereira, L. F. Veiros, S. I. Pasco, M. T. Duarte, S. Namorado and R. T. Henriques, *Inorg. Chem.*, 2007, **46**, 6880.
- 87 J. m. Assour and W. K. Kahn, *J. Am. Chem. Soc.*, 1965, **87**, 207.
- 88 J. M. Assour, *J. Am. Chem. Soc.*, 1965, **87**, 4701.
- 89 F. A. Walker, *J. Am. Chem. Soc.*, 1970, **92**, 4235.
- 90 G. N. La Mar and F. A. Walker, *J. Am. Chem. Soc.*, 1973, **95**, 1790.
- 91 F. A. Walker, *J. Magn. Reson.*, 1974, **15**, 201.
- 92 S. Van Doorslaer and A. Schweiger, *Phys. Chem. Chem. Phys.*, 2001, **3**, 159.
- 93 S. Van Doorslaer and E. Vinck, *Phys. Chem. Chem. Phys.*, 2007, **9**, 4620.
- 94 J. S. Griffith, *Discuss. Faraday Soc.*, 1958, **26**, 81.
- 95 L. M. Engelhardt and M. Green, *J. Chem. Soc., Dalton Trans.*, 1972, 724.
- 96 M. Iwaizumi, Y. Ohba, H. Iida and M. Hirayama, *Inorg. Chim. Acta*, 1984, **82**, 47.
- 97 C. J. Groombridge, L. F. Larkworthy, A. Marecaux, D. C. Povey, G. W. Smith and J. Mason, *J. Chem. Soc., Dalton Trans.*, 1992, **3125**.
- 98 B. N. Figgis, *Introduction to Ligand Fields*, John Wiley & Sons, New York, 1966.